euronoise

SH surface wave in multi-cracked solids

Olivier Poncelet, Stanislav Golkin, Christophe Aristegui, Mihai Caleap and Alexander Shuvalov

LMP, UMR CNRS 5469, Université Bordeaux I, 351, cours de la Libération, 33405 Talence, France
c.aristegui@lmp.u-bordeaux1.fr

Basing on the effective-medium approach, we calculate and analyze the dispersion spectrum of coherent SH waves in a halfspace containing random and uniform distribution of cylindrical cavities within finite depth beneath the surface. The scattering-induced dispersion and attenuation are coupled with the effect of a surface waveguide filled with scatterers. As a result, the obtained spectrum bears certain essential particularities in comparison with the standard Love-wave pattern. Simple analytical estimates enable a direct evaluation of the concentration of scatterers from the dispersion data. The results present a first step towards describing coherent wave propagation in solids with multi-cracked surface damage.

1 Introduction

The paper is concerned with the shear horizontal (SH) wave propagation in an isotropic halfspace containing multiple scatterers near its free surface. At this first stage of the study which is ultimately aimed at describing multi-cracked solids, a relatively simple case of scatterers represented by cylindrical cavities is considered. The cavities reduce the velocity and thus create a surface waveguide. An intrinsic frequency dispersion due to the scattering is superposed with that due to the wave trapping beneath the surface. An evident analogy with the Love waves invites using a dynamic-homogenization approach recently developed in [1]. It replaces the actual material with scatterers by an appropriate 'effective' one, whose elastic parameters with respect to the coherent SH wave motion are spatially constant but frequency dispersive and complex-valued. Basing on this approach, we calculate the dispersion spectrum of SH waves in a given halfspace and examine its particular properties.

2 Background

Suppose that mutually parallel cylindrical cavities of the radius a are distributed randomly and uniformly under the free surface of an isotropic halfspace up to a certain depth h ($\gg a$), see Fig. 1. The concentration ϕ of cavities over the layer of thickness h is assumed small. In view of the coherent SH wave propagation with frequency ω in the direction orthogonal to the axis of cavities [3, 4], the given medium may be seen as a transversely isotropic homogeneous layer of the effective material bonded to a substrate of the matrix material. Denote the density and the shear modulus of the matrix by ρ_2 and μ_2. The density ρ_1 and the shear modulus μ_1 of the layer depend on the concentration ϕ and on the scattering dispersion parameter

$$\widetilde{\omega} = \omega s_2 a, \tag{1}$$

where $s_2 = \sqrt{\rho_2/\mu_2}$ is the slowness of the bulk shear wave in the matrix material. According to [1], this dependence is as follows:

$$\begin{aligned} \rho_1(\widetilde{\omega}) &= \rho_2(1-\phi)\left[1+\phi r(\widetilde{\omega})\right], \\ \mu_1(\widetilde{\omega}) &= \frac{\mu_2}{1+2\phi}\left[1+\phi m(\widetilde{\omega})\right], \end{aligned} \tag{2}$$

where $r(\widetilde{\omega})$ and $m(\widetilde{\omega})$ are certain complex-valued functions, which turn to zero along with their first derivatives at $\widetilde{\omega}=0$. They are defined in full in [1]. To the leading order in low frequency such that $\widetilde{\omega}^2 \ln\widetilde{\omega} \ll 1$,

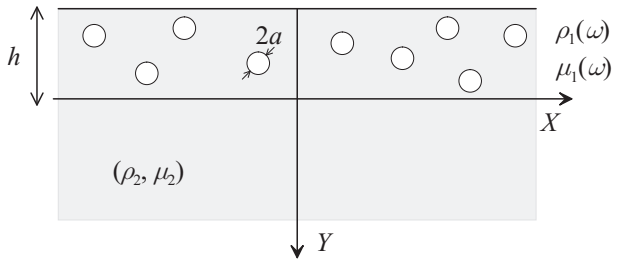

Figure 1: Geometry of the problem.

$$\begin{aligned} r(\widetilde{\omega}) &= -\tfrac{1}{2(1-\phi)}\widetilde{\omega}^2\Big\{[\ln\widetilde{\omega}+O(1)]+i\Big[-\tfrac{\pi}{2}+O\Big(\widetilde{\omega}^2\ln\widetilde{\omega}\Big)\Big]\Big\}, \\ m(\widetilde{\omega}) &= \tfrac{1}{1+2\phi}\widetilde{\omega}^2\Big\{[\ln\widetilde{\omega}+O(1)]+i\Big[-\tfrac{\pi}{2}+O\Big(\widetilde{\omega}^2\ln\widetilde{\omega}\Big)\Big]\Big\}, \end{aligned} \tag{3}$$

where the next-order terms $O(\cdot)$ in $r(\widetilde{\omega})$ and $m(\widetilde{\omega})$ are different. Note that $\operatorname{Im} r(\widetilde{\omega}) > 0$ and $\operatorname{Im} m(\widetilde{\omega}) < 0$ in agreement with the sign of dissipation.

By Eqs. (2) and (3), the complex-valued slowness of shear bulk wave in the layer $s_1(\widetilde{\omega}) = \sqrt{\rho_1(\widetilde{\omega})/\mu_1(\widetilde{\omega})}$ is

$$s_1(\widetilde{\omega}) = s_2\sqrt{(1-\phi)(1+2\phi)\,\frac{1+\phi r(\widetilde{\omega})}{1+\phi m(\widetilde{\omega})}}. \tag{4}$$

For small $\widetilde{\omega}$, it follows that

$$\begin{aligned} c_1(\widetilde{\omega}) &= c_2\frac{1}{\sqrt{(1-\phi)(1+2\phi)}}\times \\ &\qquad \left\{1+\frac{3\phi}{4(1-\phi)(1+2\phi)}\widetilde{\omega}^2\left[\ln\widetilde{\omega}+O(1)\right]\right\}, \\ \operatorname{Im} s_1(\widetilde{\omega}) &= s_2\frac{3\pi\phi}{8\sqrt{(1-\phi)(1+2\phi)}}\widetilde{\omega}^2\left[1+O\left(\widetilde{\omega}^2\ln\widetilde{\omega}\right)\right], \end{aligned} \tag{5}$$

where $c_2 = s_2^{-1}$ and $c_1(\widetilde{\omega}) = \operatorname{Re}\left[s_1^{-1}(\widetilde{\omega})\right]$ are the phase velocities. Obviously the layer and substrate (matrix) parameters differ in the measure of concentration of scatterers ϕ, so the overall effect in question is weak in the measure of small ϕ.

3 Overview of the dispersion spectrum

The guided waves are sought in the form $u_z(x,y) = U(y)\exp\left[i\omega(s_x x - t)\right]$, where the frequency ω is kept real. Taking into account the traction-free condition at the upper surface and the continuity at the bonded interface yields the dispersion equation for s_x^2,

$$i\tan\left(\omega h\sqrt{s_1^2(\omega)-s_x^2}\right) = \frac{\mu_2}{\mu_1(\omega)}\sqrt{\frac{s_2^2-s_x^2}{s_1^2(\omega)-s_x^2}}. \tag{6}$$

In contrast to the standard Love-wave case (e.g. [2]), the layer parameters s_1^2 and μ_1 are dispersive and also complex, hence the resulting dispersion branches $s_x^{(n)}(\omega)$, $n = 0,\ 1, ...,$ have real and imaginary parts. The appropriate ('physical') solutions decay into the depth of the substrate and along the propagation direction, thus satisfying the conditions $\operatorname{Im} s_{y2}^{(n)} = \operatorname{Im}\sqrt{s_2^2 - s_x^{(n)2}} \geq 0$ $\operatorname{Im} s_x^{(n)} \geq 0$ for $\operatorname{Re} s_x^{(n)} > 0$ and the axes X, Y as in Fig. 1. Note a difference with a leaky wave, whose horizontal decay is accompanied by increase into the depth. It is worth pointing out to this end that the Love-wave dispersion equation with real material constants admits only real slowness solutions for real ω, so that the complex branches $s_x^{(n)}(\omega)$ in hand arise as a perturbation of just these real solutions (it is in contrast with the case of Lamb waves admitting complex conjugated slowness branches for non-absorbing plates).

Figs. 2 and 3 show the calculated spectrum for two different values of concentration of cavities with the radius $a = 0.06mm$, which are distributed within the layer of thickness $h = 1$ mm in the aluminum matrix with $\rho_2 = 2.7$ g/cm^3 and $\mu_2 = 26.45$ GPa. The results are displayed in terms of the phase velocity and the attenuation

$$c^{(n)} = \operatorname{Re}\left(1/s_x^{(n)}\right),\ \alpha^{(n)} = \omega \operatorname{Im} s_x^{(n)}, \qquad (7)$$

which are plotted as functions of $\widetilde{\omega} = ka$ and of ωh. The dashed line is the phase velocity c_2 for the matrix material (substrate), the dotted lines are the phase velocity $c_1(\omega)$ and the attenuation $\alpha_1(\omega) = \omega \operatorname{Im} s_1$ of the shear bulk wave for the effective layer material.

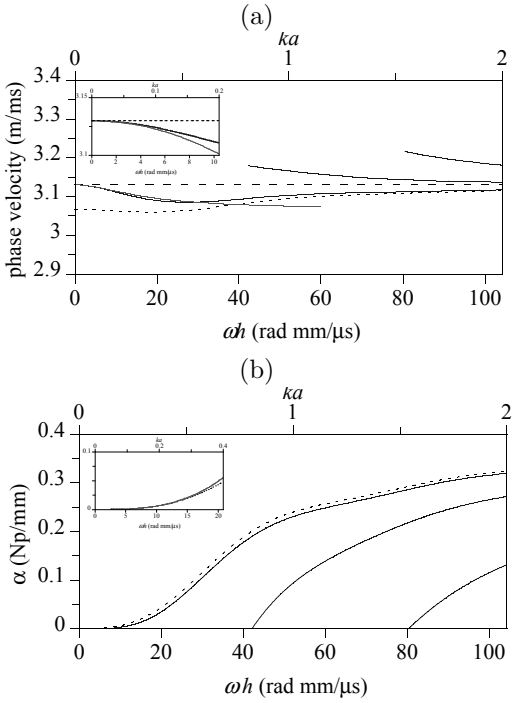

Figure 2: The branches of (a) phase velocity $c^{(n)}(\omega)$ and (b) attenuation $\alpha^{(n)}(\omega)$ for the concentration of scatterers $\phi = 4.52\%$. The notations are explained in the text.

4 Discussion

4.1 Fundamental branch

It is noted that the 'waveguiding' dispersion governed by $\omega s_0 h$ is h/a times stronger than that due to the scattering dispersion parameter $\widetilde{\omega}$. Given $h/a \gg 1$, the fundamental phase-velocity curve $c^{(0)}(\omega)$ for small $\widetilde{\omega}$ can be approximately defined by via confining in Eq. (6) the effective parameters $s_1^2(\omega)$ and $\mu_1(\omega)$ by their statically averaged values $s_1^2(0) = s_2^2(1-\phi)(1+2\phi)$ and $\mu_1(0) = \mu_2/(1+2\phi)$, see Eq. (2). For another long-wave scale which is $(\omega h s_2)^2 \ll 1$, the leading order of an explicit expansion gives

$$c^{(0)}(\omega) \approx c_2\left[1 - \frac{1}{2}(\omega h s_2)^2 \frac{\phi^2(1-2\phi)^2}{(1+2\phi)^2}\right]. \qquad (8)$$

Both long-wave approximations are shown by gray lines in Figs. 2a, 3a and the insets in there.

Starting from high enough frequency, the fundamental branch $c^{(0)}(\omega)$ trails above the bulk-wave velocity in the layer $c_1(\omega)$. This is as usual. However, for the case in hand $c_1(\omega)$ is dispersive. According to Eq. $(5)_1$, it reaches minimum at about the minimum point $\widetilde{\omega} = e^{-1/2} \approx 0.6$ of the function $\widetilde{\omega}^2 \ln\widetilde{\omega}$ and then curves upwards. Hence so does the branch $c^{(0)}(\omega)$.

Due to $h/a \ll 1$, the attenuation curve $\alpha^{(0)}(\omega)$ corresponding to the fundamental branch is close from below to the attenuation $\alpha_1(\omega) = \omega \operatorname{Im} s_1(\omega)$ of shear bulk waves in the layer. For $\widetilde{\omega}^2 \ln\widetilde{\omega} \ll 1$, the latter is approximated through Eq. $(5)_2$, so that

$$\alpha^{(0)}(\omega) \lessapprox \alpha_1(\omega) \approx \frac{3\pi\phi\widetilde{\omega}^3}{8a\sqrt{(1-\phi)(1+2\phi)}}, \qquad (9)$$

see gray lines in the zoomed insets to Figs. 2b and 3b.

4.2 Higher-order branches

Scattering-induced dispersion and attenuation underlie an unusual behavior of the higher-order branches ($n > 0$). Commonly the origin points (cutoffs) of higher-order velocity curves simply correspond to the grazing propagation in the substrate and hence all lie on the line $c^{(n)}\left(\omega_c^{(n)}\right) = c_2$, where $\omega_c^{(n)}$ denotes the cutoff frequency. In the present case, it is not so.

We recall that a formal solution $s_x^{(n)}(\omega)$ of the (complex) dispersion equation (6) admits either signs of the imaginary parts of $s_{y2}^{(n)}(\omega)$ and $s_x^{(n)}(\omega)$, and it is their positiveness which selects the 'physical' part of the branch $s_x^{(n)}(\omega)$. For a purely elastic substrate (with real s_2), $\operatorname{Im} s_{y2}^{(n)}$ and $\operatorname{Im} s_x^{(n)}$ turn to zero simultaneously. Thus the cutoff points $(\omega_c^{(n)},\ s_x^{(n)}\left(\omega_c^{(n)}\right))$ of the higher-order branches are defined as the points of 'nonphysical/physical' crossover $\operatorname{Im} s_x^{(n)}\left(\omega_c^{(n)}\right) = 0$, which implies that $c^{(n)}\left(\omega_c^{(n)}\right) > c_2$. That is why the cutoffs lie above the substrate velocity c_2.

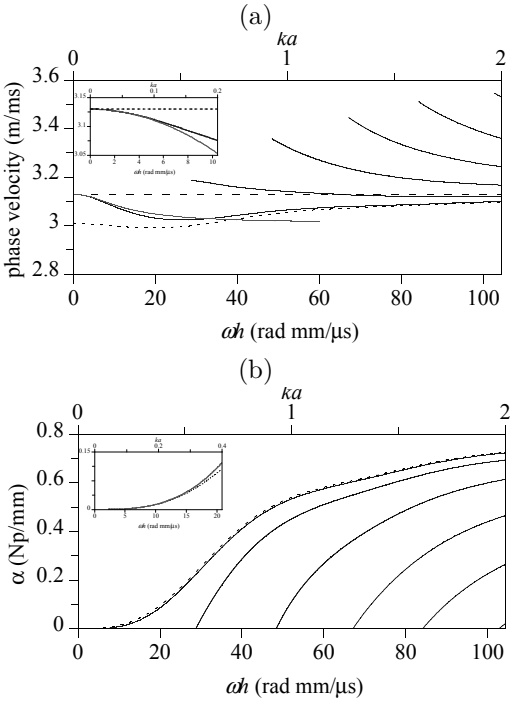

Figure 3: The branches of (a) phase velocity $c^{(n)}(\omega)$ and (b) attenuation $\alpha^{(n)}(\omega)$ for the concentration of scatterers $\phi = 10.18$ %.

The onsets of a few first higher-order branches shown in Figs. 2 and 3 can be approximately related by a simple expression

$$\omega h \,\mathrm{Re}\sqrt{s_1^2(\omega) - s_x^{(n)2}(\omega)} \approx \pi n, \tag{10}$$

which implies a small imaginary part of the left-hand side of Eq. (6). For the cutoff values $\omega_c^{(n)}$ and $c_c^{(n)} \equiv c^{(n)}\left(\omega_c^{(n)}\right)$, Eq. (10) reduces to

$$\omega_c^{(n)} h \sqrt{\mathrm{Re}\, s_1^2 - \frac{1}{c_c^{(n)2}}} \approx \pi n, \tag{11}$$

The cutoff velocity $c_c^{(n)}$ in Figs. 2a and 3a increases with growing branch number n; however, it can be shown to reach a plateau for greater n which are beyond the displayed frequency band.

In turn, the attenuation branches $\alpha^{(n)}(\omega)$ for $n > 0$ start from zero value at the successive cutoff frequencies $\omega_c^{(n)}$ and then increase in a similar manner. Accordingly to Eq. (10), each next attenuation branch lies below the preceding one, while the distance between them at a fixed frequency ω reduces with growing ω, see Figs. 2b and 3b.

5 Conclusions

The effective-medium approach has been used for calculating the spectrum of coherent SH waves in a halfspace which contains random distribution of cylindrical cavities within finite depth beneath the surface. It is shown that the effect of the dispersion and attenuation caused by the scattering leads to some unusual spectral features, which are different from the standard pattern of Love-wave spectrum in coated elastic solids. Simple analytical estimates enable a direct evaluation of the concentration of scatterers from the dispersion data.

References

[1] C. Aristégui, Y. C. Angel, "Effective material properties for shear-horizontal acoustic waves in fiber composites, *Phys. Rev. E 75*, 056607 (2007)

[2] B.A.Auld, Acoustic Fields and Waves in Solids. Wiley-Interscience Publication, New York, 1973.

[3] P. C. Waterman, R. Truell, "Multiple scattering of waves," *J. Math. Phys. 2*, 512-537 (1961).

[4] Y. C. Angel, Y. K. Koba, "Complex valued wavenumber, reflection and transmission in an elastic solid containing a cracked slab region," *Int. J. Solids Struct. 35*, 573-592 (1998).